## Title

Control of stem-cell niche establishment in Arabidopsis flowers by REVOLUTA and the LEAFY-RAX1 module

## Authors

Denay Grégoire[1,2,*], Tichtinsky Gabrielle[1], Le Masson Marie[1], Chahtane Hicham[1,§], Huguet Sylvie[3,4], Lopez-Vidriero Irene[6], Wenzl Christian[5], Franco-Zorrilla José Manuel[6], Simon Rüdiger[2], Lohmann Jan U.[5], and Parcy François[1,*]

## Affiliations

1 - Univ. Grenoble Alpes, CNRS, CEA, INRA, BIG-LPCV, 38000 Grenoble, France

2 - Institute for Developmental Genetics, Heinrich Heine University, Düsseldorf, Germany.

3 - Institute of Plant Sciences Paris Saclay IPS2, CNRS, INRA, Université Paris-Sud, Université Evry, Université Paris-Saclay, Bâtiment 630, 91405 Orsay, France.

4 - Institute of Plant Sciences Paris-Saclay IPS2, Paris Diderot, Sorbonne Paris-Cité, Bâtiment 630, 91405, Orsay, France.

5 - Centre for Organismal Studies, Heidelberg University, Heidelberg, Baden-Württemberg, Germany.

6 - Genomics Unit, Centro Nacional de Biotecnología, Consejo Superior de Investigaciones Científicas, 28049 Madrid, Spain.

## Additional Footnotes

§ - Present address: Department of Plant Biology, University of Geneva, 30 Quai Ernest-Ansermet-Sciences III, 1211, Geneva 4, Switzerland.

* - Corresponding authors: francois.parcy@cea.fr; gregoire.denay@hhu.de

## Abstract

Plants retain the ability to produce organs throughout their life by maintaining active stem cell niches called meristems. The shoot apical meristem (SAM) is responsible for the growth of aerial plant structures. In *Arabidopsis thaliana*, the SAM initially produces leaves during the vegetative phase and later flowers during reproductive development. In the early stages of floral initiation, a group of cells first emerges from the SAM to form a stereotypically organized meristematic structure on its flank. However, the molecular mechanisms underlying the acquisition of this specific meristematic organization remain elusive. We show here that the transcription factors LEAFY (LFY) and REVOLUTA (REV) control two partially redundant pathways controlling meristematic organization in early flower primordia. We found that LFY acts through the transcription factor REGULATOR OF AXILLARY MERISTEM1 (RAX1) and we provide mechanistic insights in how RAX1 allows meristem identity establishment in young flowers. Our work provides a molecular link between the processes of meristem formation and floral identity acquisition in the nascent flower.

## Introduction

Plants retain the capacity to initiate new organs throughout their life. To this end, they maintain self-sustaining pools of stem cells in organized niches called meristems. The SAM gives rise to most post-embryonic aerial organs thanks to stem cells present in its central zone (CZ). These cells are maintained in an undifferentiated state by a genetic network including the two transcription factors (TF) WUSCHEL (WUS) and SHOOTMERISTEMLESS (STM). WUS is expressed in the organizing centre (OC) of the SAM, located a below the CZ where it migrates to repress cell differentiation programs (Mayer et al., 1998; Yadav et al., 2011, 2013, 2010). STM is widely expressed in the SAM and acts at least in part *via* the regulation of the CK levels (Endrizzi et al., 1996; Jasinski et al., 2005; Lenhard et al., 2002; Yanai et al., 2005). Maintenance of the stem cell pool in the SAM involves a regulatory feedback loop between WUSCHEL (WUS) and the CLAVATA (CLV) signalling module (Schoof et al., 2000; Gaillochet et al., 2015; Brand et al., 2000). WUS induces the expression of the stem cell marker *CLAVATA3* (*CLV3*) in the CZ (Brand et al., 2002). *CLV3* encodes a signalling peptide that binds its CLV1 receptor in the cells surrounding the OC (Ogawa et al., 2008), leading to negative regulation of WUS (Brand et al., 2000). This regulatory loop controls stem cell homeostasis by regulating the size of the stem cell niche. CK is also important for meristem maintenance by regulating both *WUS* and *CLV3* expression and promoting stemness (Zhao et al., 2010; Gordon et al., 2009). In the peripheral zone of the SAM, primordia develop as leaves during the vegetative phase and as flowers after floral transition at sites primarily determined by auxin maxima. Both leaf and flower primordia initiation require an initial downregulation of the *KNOX* genes *STM* and *KNAT1*. However, during flower development, expression of *KNOX* and of genes controlling stem cell fate such as *WUS* and *CLV3* are regained at a later stage. Indeed, at stage 2 (referred to here as flower meristem, FM), the flower primordia become patterned with distinct meristematic domains: they acquire *WUS* expression domain, marking the establishment of the OC, closely followed by that of *CLV3* marking the CZ, and of *UNUSUAL FLORAL ORGANS* (*UFO*), another gene expressed both in the SAM and in stage 2 FM (Yoshida et al., 2011; Samach et al., 1999; Wilkinson and Haughn, 1995).

In parallel to its development as a meristem, the flower primordium acquires its floral fate. Several flower meristem identity genes (*LFY*, *APETALA1*, *CAULIFLOWER* and other MADS-box TF) confer to the nascent FM its flower specific features: determinate growth, whorled phyllotaxis, whorled pattern of floral organ identity genes expression (Chandler and Werr, 2014; Kaufmann et al., 2010; Denay et al., 2017) . Among those, *LFY* is expressed first and throughout floral development. It acts as a key floral regulator, building on the meristematic pre-patterning defined by *WUS* or *UFO* to locally induce floral organ identity genes (Laux et al., 1996; Lohmann et al., 2001; Parcy et al., 1998).

How the floral primordium grows and acquires its meristematic organization still remains elusive (Denay et al., 2017). The proposed mechanisms involve a combination of growth and hormone signalling (Gruel et al., 2016), but the executive transcriptional signals remain largely uncharacterized. An efficient way to coordinate the establishment of the meristematic organization with floral fate acquisition is probably to couple both processes. LFY was proposed to participate in both (Moyroud et al., 2010) and genetic evidence have indeed accumulated, documenting its contribution to meristem emergence (Yamaguchi et al., 2013; Wu et al., 2015; Sawa et al., 1999; Chahtane et al., 2013). This function is particularly obvious in rice where LFY participates in tiller growth and panicle meristem development, and in legumes where LFY triggers compound leaf development; all processes requiring the acquisition of meristematic features (Moyroud et al., 2010). In Arabidopsis, such function for LFY remains cryptic as *lfy* mutants develop lateral structures such as meristems and leaves, suggesting LFY might act redundantly with other pathways (Moyroud et al., 2010). However, constitutive expression of LFY triggers ectopic flower production in the axils of rosette leaves or cotyledons (Chahtane et al., 2018; Sayou et al., 2016). This effect on floral meristem production can even be uncoupled from floral identity by impairing LFY dimerization. Expression of a LFY variant triggers the development of precocious or ectopic inflorescence meristems instead of flowers in the axil of rosette leaves, through the induction of the R2R3 TF REGULATOR OF AXILLARY MERISTEMS1 (RAX1) (Chahtane et al., 2013). Thus, in Arabidopsis too, LFY appears to be able to trigger meristem formation. Whether the LFY-RAX1 module that acts at the axil of rosette leaves is also active in flowers is unknown: RAX1 is expressed in flower meristems but *rax1* mutants do not exhibit any floral

phenotype (Keller et al., 2006; Müller et al., 2006). Just as for LFY, we surmised that a role of RAX1 on floral meristem might be masked by redundancy with other pathways.

Such pathways might involve the HD-ZIPIII family of TFs that is linked to *de novo* meristem formation in aerial tissues. Triple mutants of *revoluta* (*rev*) *phabulosa phavoluta* fail to form an embryonic SAM (Prigge et al., 2005) and single *rev* mutants show pleiotropic defects (Otsuga et al., 2001; Talbert et al., 1995). These defects include failure to form axillary stems and occasionally flowers, resulting in the formation of filaments or of flowers similar to those of weak *wus* mutants (Otsuga et al., 2001; Laux et al., 1996). Additionally, REV was shown recently to be an essential component of axillary shoot meristem formation by stimulating the expression of *STM* in the leaf axils and determining adaxial fate in young developing organs (Shi et al., 2016; Caggiano et al., 2017; Zhang et al., 2018).

Because *REV* appears as a possible candidate to act in parallel with the *LFY/RAX1* pathway in flowers, we combined mutations in both pathways to study their potential role in the acquisition of the meristematic structure of the flower primordium. We show that REV and the LFY-RAX1 module control the establishment of meristematic domains in flowers and that RAX1 may act in part by repressing *CLV1* expression in the young flower bud, thereby enabling proper *WUS* expression and meristem patterning. This work reveals a molecular coupling between the establishment of the floral meristem structure and the acquisition of its floral identity through the action of LFY in both processes.

## Results

### *LFY and REV act in parallel pathways during flower meristem development*

To gain insight into the role of LFY in early floral meristem development, we analysed the effect of *lfy* mutations in the *rev* mutant background. As *LFY* and *REV* are genetically linked, we used CRISPR/Cas9 to target the third and ninth exons of the *REV* gene (Supplemental Figure 1A) to simplify the isolation of *lfy rev* double mutants. Several *rev* alleles were recovered in a *pWUS:2xVENUS-NLS:tWUS* reporter (*pWUS:Venus;* Supplemental Figure 2A), carrying insertions or deletions leading to premature stop codons in the third exon (Supplemental Figure 1A). These plants showed similar phenotypes to the previously described *rev-6* mutant allele

(Otsuga et al., 2001). One representative line (thereafter named *rev-c1*) was further characterized: its leaves were slightly over-curved downward, the number of axillary stems was reduced, 20% of flowers lacked internal whorls, and some rare flowers were replaced by filaments (Supplemental Figure 3 A,B).

We then crossed this line still containing the REV-targeting CRISPR construct into *lfy-12/+* mutants. In the F2, we observed plants with typical *lfy* and *rev* mutant aspects as well as plants showing a dramatically enhanced phenotype with nearly all flowers replaced by small filamentous structures. These plants were clearly distinct from *rev*-like plants that bear distorted flowers (sometimes lacking the inner whorls) and from *lfy* mutants that lack flowers but display fully developed lateral structures (secondary shoots or shoot/flower intermediates) (Figure 1A-D). We selected one plant with a clear *rev* phenotype that was heterozygous for the *lfy-12* allele, and which no longer carried the CRISPR construct. Sequencing of *REV* around the site of Cas9 nuclease activity in this plant revealed a homozygous one base deletion resulting in a premature stop codon in the third exon of *REV*. This mutation was called *rev-c4* (Supplemental Figure 1A). Co-segregation analysis after one back-cross to wild-type showed that the newly observed filamentous phenotype is specific to *lfy-12 rev-c4* double mutants (Supplemental Table 1).

The growth of short determinate filaments instead of flowers suggests that the *lfy-12 rev-c4* mutant phenotype might arise from a failure to establish a functional floral meristem. To test this hypothesis, we analysed the activity of the *pWUS:Venus* reporter in inflorescences of the *rev-c4* and *lfy-12 rev-c4* mutants (Figure 1E-L). In wild-type plants, *WUS* expression is detectable from late stage 1 onwards, when the flower primordium forms a bulge; this expression is, however, very weak and restricted to only a few cells (Supplemental Figure 2D). At early stage 2, *WUS* expression is enhanced in the centre of the flower meristem (Supplemental Figure 2E) and absent from the peripheral zone and the L1 layer in almost all observed flowers (32/33). However, it is strongly expressed in the L2 of flower meristems (Supplemental Figure 2E) in contrast to the SAM, where *WUS* expression is restricted to the L3. These observations contrast with some previous reports of *WUS* promoter activity in the L2 of the SAM and the L1 of FMs (Yadav et al., 2011), but are in accordance with several independent data obtained by *in situ* hybridization (Yadav and Reddy, 2012; Mayer et al., 1998; Leibfried et al., 2005). Similar to wild-type

plants, the *rev-c4* mutants showed *WUS* expression in flower primordia at stage 2. However, when combined with the *lfy-12* mutation, the WUS-Venus signal was strongly altered in primordia (Figure 1E-N): more than 50% of the primordia at stage 2 or more advanced stages lacked detectable *WUS* expression (Supplemental Figure 4) and about 20% of the primordia showed *WUS* expression restricted to the axil of the developing filament (Figure 1I-L, Supplemental Figure 4C).

The presence of filaments that fail to establish a floral stem cell niche in the *lfy rev* double mutant suggests that *REV* and *LFY* act partially redundantly to build a functional floral meristem. Thus, the *rev* mutant represents a sensitized background suitable to investigate LFY's molecular function in the formation of the floral stem cell niche.

*The LFY target RAX1 contributes to floral meristem development with REV*

Next we wondered whether the LFY-RAX1 module acting on axillary meristems (Chahtane et al., 2013) also participates in FM meristematic organisation. It was previously shown that *RAX1* mRNA levels in inflorescences are not altered by mutations in *lfy* but that RAX1 expression is increased in plants expressing a constitutively active form of LFY, which is derived from a fusion between LFY and the VP16 *trans*-activation domain under the control of *LFY* promoter (LFY-VP16) (Chahtane et al., 2013; Parcy et al., 1998). To study the spatial effect of LFY-VP16, we compared *RAX1* expression between wild-type plants and plants expressing LFY-VP16 using both *in situ* hybridisation and a *RAX1:GUS* transcriptional reporter (Supplemental Figure 5). We found that in the presence of LFY-VP16, *RAX1* expression was stronger in early floral meristems and broader in inflorescences, confirming that LFY can promote *RAX1* expression in these tissues.

Next, we probed the role of *RAX1* during FM emergence. Since *rax1* mutants have no floral defects (Keller et al., 2006; Müller et al., 2006), we introduced the *rax1-3* mutation into the *rev-6* background. In this case, the *rev-6* L*er* allele was backcrossed 3 times into Col-0. *rev-6* [Col-0] displayed a higher proportion of flowers either lacking floral organs (63%) or replaced by filaments (27%) (Figure 2I) than reported for *rev-6* in L*er* (12% of flowers presenting defects) (Otsuga et al., 2001) or observed in the *rev-c1* allele described above (20% of flowers lacking internal whorls, and 1% is replaced by filaments) (Supplemental Figure 3B). The presence of the

*rax1-3* mutation considerably enhanced the *rev-6* phenotypes (Figure 2). *rev-6 rax1-3* plants produced only a few fertile flowers (1 to 2 per plant on average) and the proportion of filaments was much higher than in *rev-6* (75% of flowers replaced by filaments and 22% lacking internal whorls). Also, the plants seldom formed axillary stems (Supplemental Figure 6A-D) and main axis growth was prolonged, resulting in the formation of an abnormally long main stem.

Analysis of *rev-6 rax1-3* inflorescences by scanning electron microscopy revealed either filaments or 'empty flowers' only made of a whorl of sepals lacking a meristematic dome (Figure 2 E-H,J-M). Both phenotypes suggested a failure to establish a flower meristem of adequate size to allow development of all four whorls of organs. The strong genetic interaction between *rax1* and *rev* mutations was further illustrated by the following observations: 1) the *rax1-3* mutation behaved semi-dominant in the *rev-6* background (Supplemental Figure 7): *rev-6 rax1-3*/*RAX1* plants displayed for instance less axillary stems than *rev-6* mutants. 2) In short-day conditions, where the *LFY* pathway is less active (Blázquez et al., 1997), the *rev-6* phenotype was enhanced, with inflorescences essentially made of filaments subtended by bract primordia. In these growth conditions, the *rax1-3 rev-6* phenotype was drastic: filaments were extremely reduced and stipule-like organs became visible on the flanks of rudimentary bracts (Supplemental Figure 8).

In conclusion, although the single *rax1* mutation does not display any flower phenotype, our results using the *rev-6* background show that RAX1 and REV both act to regulate development of early flower primordia.

*RAX1 and REV are required for FM meristematic structure*

The development of flowers lacking internal whorls or of filaments suggested that the flower meristematic structure is not properly established or maintained in *rax1 rev* mutants. To characterize possible meristematic defects of these double mutants, we monitored the expression of the *CLV3* and *WUS* meristem patterning markers using *in situ* hybridization. Whereas the expression of *CLV3* and *WUS* was not altered in the SAM, they were strongly reduced or even absent in some *rax1-3 rev-6* "flower" primordia (Supplemental Figure 9). Other primordia displayed a detectable and normally localized *WUS* and *CLV3* expression consistent with the fact that *rax1 rev*

mutants showed a mixture of severely affected structures (empty flowers or filaments) as well as some more normal flowers (Figure 2).

In order to more finely track the establishment of the floral OC over developmental time, we introduced CRISPR/Cas9 constructs targeting both *RAX1* and *REV* in the *pWUS:Venus* reporter line. We validated the isolation of *rax1* and *rev* single mutants and *rax1 rev* double mutants by phenotypic characterization and genotyping (Supplemental Figures 1 and 3). We recovered several types of mutations that all resulted in frameshifts at the same sequence site, which led to stop codons at different downstream positions (*rev-c2*, *-c3* and *rax1-c1*, *-c2* and *-c3*; Supplemental Figure 1). For the *rax1 rev* double mutant, we studied the progeny of a double heteroallelic plant (*rax1-c2/3 rev-c2/3*). In this *rax1-c2/3 rev-c2/3* double mutant, the *pWUS:Venus* signal was weaker in the first few primordia than in either *rax1-c1* or *rev-c1* single mutants, but still detectable (Figure 3A-C). However, the main effect of this mutation combination was an expansion of the *WUS* expression domain in young flowers. Such ectopic *WUS* expression was observed in only 12% (N=40) of *rax1-c1* flowers, while single *rev-c1* mutant showed ectopic *WUS* expression in 75% (N=35) of observed flowers, either restricted to the apical domain of the L1 (44%) or throughout the L1 (31%). In contrast, double mutants exhibited ectopic *WUS* expression in almost all observed flowers (95%, N=23), in the apical domain of the L1 and throughout the L1 in 30% and 65% of the flowers, respectively (Figure 3J-L', O). Additionally, the *WUS* expression domain appeared shifted apically in the *rev-c1* mutant and to a higher extent in the double mutant where *WUS* expression was restricted to the topmost 3-5 cell layers, while it reached much deeper layers in *rax1-c1* and WT (Figure 3D-L'). The SAM was also considerably enlarged in double mutants, however we could not detect any defect in *WUS* expression there (Figure 3A-C and Supplemental Figure 10).

Taken together, these data indicated that *REV* and *RAX1* are important regulators controlling both the level and spatial expression of *WUS* in the centre of emerging flower primordia. While the contribution of *RAX1* may be hidden due to redundancy in a single mutant situation, its role became clear when *REV* function was also compromised: double mutants showed a reduction in *WUS* expression levels combined with a dramatic expansion of the *WUS* expression domain in the L1 and the peripheral domains of floral primordia. Since the proportion of flowers showing

expression of *WUS* in the peripheral zone was strongly increased in double mutants, we hypothesised that *RAX1* plays a more specific role in preventing OC expansion in the peripheral zone while *REV* acts mostly in positioning the OC below the L1. The defects in OC positioning, and thus FM organization, is likely the cause for the floral defects observed in these mutants.

*RAX1 induces WUS expression*

To understand how RAX1 regulates meristem formation, we generated plant lines expressing a mCherry-RAX1-GR (*iRAX1*) fusion protein under the control of the moderate constitutive *UBQ10* promoter (Geldner et al., 2009). The hormone binding domain of the glucocorticoid receptor (GR) allows the retention of the fusion protein in the cytoplasm and its conditional translocation to the nucleus upon dexamethasone (DEX) treatment (Padidam, 2003). RAX1 protein expression was validated by western blot (Supplemental Figure 11I). When RAX1 activity was induced over a long period of time by periodic DEX treatments, plants appeared stunted, retarded in growth and produced very small siliques with only a few seeds. Mock treated *iRAX1* plants were slightly smaller than a control transgenic line expressing mCherry-GR fusion proteins (*iMock*), indicating a residual activity of the construct in the absence of DEX (Supplemental Figure 11A-H).

In the *iRAX1* line, we could observe ectopic *WUS* expression in the L1 of young flowers as early as 6h after DEX treatment in 7 out of 12 plants (Figure 4A), while control *pWUS:Venus* plants showed normal *WUS* expression up to 24h after DEX treatment (10 out of 11 plants) (Figure 4B). This indicated that ectopic activation of RAX1 transcriptional activity in young flowers could trigger ectopic *WUS* expression throughout the FM.

*RAX1 acts on multiple signalling pathways*

In order to gain insight into RAX1 TF molecular function, we examined gene expression in response to RAX1 post-transcriptional induction in the *iRAX1* line in comparison to *iMock*. Paired-end RNA-sequencing analysis was performed on 14-day-old seedlings expressing the above-mentioned *iRAX1* line or *iMock* mock line, 4h after DEX or mock treatment, with three biological replicates for each condition, yielding libraries of 26 to 37 million reads. Principal component analysis of the top 500 variable genes across all datasets showed a clear segregation of the DEX-

299 treated RAX1 inducible line along the first component axis (Figure 5A), indicating a
300 specific transcriptome response in these samples. We identified 822 differentially
301 expressed genes (DEG; FDR ≤ 0.01, 482 down- and 340 up-regulated) in response
302 to both the treatment and the presence of RAX1 (Figure 5B, Supplementary Dataset
303 1). Gene ontology (GO) analysis showed an enrichment of genes involved in cell
304 modifications and phenylpropanoid synthesis amongst the genes up-regulated. The
305 down-regulated genes were enriched in genes involved in various immune and
306 hormone responses (Figure 5C; Supplementary Datasets 2-3).

307 *In silico prediction of putative direct RAX1 targets*

308 We aimed at identifying putative direct targets of RAX1 amongst the differentially
309 expressed genes. For this, we determined RAX1 DNA-binding properties using
310 protein-binding micro-array (PBM) (Franco-Zorrilla et al., 2014). We used the RAX1
311 protein fused to Maltose Binding Protein (MBP) and a 6-Histidine tag ($RAX1_{full}$-MBP-
312 6H) produced recombinantly in *E. coli*. The best motif obtained by PBM matches well
313 previously described Myb R2R3 motifs (Franco-Zorrilla et al., 2014) (Figure 5D).
314 Using this DNA-binding model, we determined both the best RAX1 predicted binding
315 sites (RAX1bs) and the probability of occupancy (pOcc) (Granek and Clarke, 2005)
316 by RAX1 in the genomic region of each differentially expressed gene. The scores
317 obtained for RAX1 DNA-binding model ranged from -47.87 (worst possible RAX1bs)
318 to 14.37 (best RAX1bs). In order to focus on the genes most likely to be direct
319 targets, we arbitrarily set a score threshold of 12 and a pOcc threshold of 0.2
320 corresponding to the top 51 and 33 % respectively. Based on these predictions, we
321 identified 272 genes (out of 822) as best direct targets candidates of RAX1 (Figure
322 5E, Supplementary Dataset 4). These included a set of genes with experimental
323 evidence for SAM expression (Yadav et al., 2014, 2009) (Supplemental Table 2).

324 Among the predicted RAX1 direct targets, we identified ABF2, a protein linked to
325 abscisic acid signalling, confirming previous evidence of ABF2 regulation by RAX1
326 (Kim et al., 2004; Yu et al., 2016). We also identified the transcription factors
327 ETHYLENE RESPONSE FACTOR (ERF) 1 and 2, involved in ethylene and
328 jasmonate signalling, and in pathogen response (Cheng et al., 2013). Numerous cell-
329 wall remodelling enzymes as well as the two pectin receptors WALL ASSOCIATED
330 KINASE (WAK) 1 and 2 were also identified, all of which have roles in cell growth
331 regulation (Goh et al., 2012; Hewezi et al., 2008; Liang et al., 2013; Wu et al., 2010;

Wagner and Kohorn, 2001; Kohorn et al., 2006). Finally, high-score RAX1 binding sites were detected in the *UPBEAT1* (*UPB1*) and *CLV1* genomic regions. UPB1 is involved in the control of ROS balance and was shown to control root and shoot stemness (Tsukagoshi et al., 2010; Zeng et al., 2017). The inhibition of *UPB1* and *CLV1* observed in response to RAX1 activity suggests that RAX1 may contribute in stem cell niche maintenance by repressing these genes (Supplemental Table 2).

### RAX1 *directly regulates CLV1 expression*

*CLV1,* a known negative regulator of *WUS*, was identified as a putative direct RAX1 target and was repressed over two-fold in seedlings in response to RAX1 induction. *CLV1* carries two high-score (> 12) RAX1bs in its promoter and coding sequence (Figure 6A). In order to determine if *CLV1* is a genuine target of RAX1 in the shoot apex, we analysed *CLV1* expression by qRT-PCR in mock- or DEX-treated *iRAX1* inflorescences. *CLV1* mRNA levels were mildly reduced in response to DEX treatment (Figure 6B) and this reduction was still observed in the presence of the protein synthesis inhibitor cycloheximide (CHX) indicating that this regulation is likely direct. Consistent with this result, we found that recombinantly produced $RAX1_{full}$-MBP-6H as well as a tagged truncated version of RAX1 carrying only the Myb domain ($RAX1_{myb}$-6H) were able to specifically bind oligonucleotides carrying either the best predicted RAX1bs or the one present in *CLV1 cis*-regulatory region (Figure 6C). Taken together, these results indicated that RAX1 most likely binds the *CLV1* promoter *via* its Myb domain, and is able to reduce *CLV1* expression.

## Discussion

### *REV and the LFY-RAX1 module control flower meristem development*

Since it was first proposed (Moyroud et al., 2010), several studies suggested that LFY could also be involved in the establishment of meristematic structures of FMs, in addition to its well-studied role in flower identity determination (Sawa et al., 1999; Yamaguchi et al., 2013; Wu et al., 2015; Chahtane et al., 2013; Moyroud et al., 2010). However, *lfy* mutants do initiate lateral structures on shoots, indicating that either LFY does not play any role in this process or that other pathways can compensate for the loss of LFY function. Because *rev* mutants are affected in flower initiation and meristem formation (Talbert et al., 1995; Otsuga et al., 2001; Prigge et al., 2005), we used *rev* as a sensitized background to study the role of *LFY* in FM

formation. We found that combinations of *lfy* and *rev* mutations almost completely abolished the formation of flowers, which were replaced by small filamentous organs. These structures often lacked proper *WUS* expression, a likely explanation for their failure to establish floral meristems. These results unambiguously showed that *LFY* acts in parallel with *REV* in the acquisition of meristematic features in FM.

It was proposed earlier that *LFY* ectopically induces meristem formation through the regulation of *RAX1* (Chahtane et al., 2013). Although *RAX1* is expressed in flower primordia, *rax1* single mutants do not display any floral phenotype (Keller et al., 2006; Müller et al., 2006) and it was unclear whether RAX1 participates in floral meristem initiation as it does for axillary branches. We show here that *RAX1* is a likely target of LFY in early flowers. This regulation was not detected in *lfy* mutants (Chahtane et al., 2013) likely because in this background flowers are replaced by shoot/flower intermediates that express *RAX1* through independent mechanisms, probably similar to the situation in leaf axils (Guo et al., 2015). When combined with mutations in *rev*, the loss-of-*rax1* mutations drastically enhanced flower developmental defects and many flowers were either replaced by filamentous structures or lacked internal organ whorls. The defects observed in *rax1 rev* mutants were milder than that of *lfy rev* mutants either because the *rax1* alleles used here contain mutations in the C-terminal part of the proteins, which can retain some activity, or because LFY regulates additional genes involved in meristem formation such as A-type ARRs (Chahtane et al., 2013).

*Filaments likely result from failed flower meristem establishment*

Filaments replacing flowers in *lfy rev* or *rax1 rev* double mutants are structures that do not differentiate further and seem to have a determinate growth. To characterize those structures, we monitored the expression of *WUS* and *CLV3* as meristematic markers for the OC and stem cell zone, respectively. We found that some flowers of the *rax1-3 rev-6* mutant lacked the expression of both *WUS* and *CLV3* in the first flower development stages where they normally appear. In weaker mutant contexts (such as *rax1-c2/3 rev-c2/3*), we observed lower *WUS* expression but shifted upwards in the L1 and underlying layers, indicating that both *RAX1* and *REV* are involved in the regulation of *WUS* expression and its exclusion from the L1. However, RAX1 specifically prevents *WUS* expression in the flower PZ, including in the L1. When RAX1 activity was ectopically induced, *WUS* expression became present

throughout the flower primordia. Since *REV* is not expressed in the PZ of flower primordia (Otsuga et al., 2001), we conclude that RAX1 likely induces *WUS* expression independently of *REV*. *RAX1* and *REV* are thus required for *WUS* activation and the proper definition of the FM domains, and filaments appeared to result either from loss of primordia meristematic organization leading to the development of a determinate structure, or from the consumption of the stem-cell pool, resulting in flowers lacking internal whorls.

Altogether these data indicate a role of *RAX1* downstream of *LFY* in parallel to *REV* to regulate the acquisition or the maintenance of the flower meristem structure.

*SAM size is increased when filaments replace flowers*

In addition to their role in flower primordia, LFY/RAX1 and REV showed a synergistic effect on restricting the size of the OC and the SAM. The size of the OC in the double *rax1 rev* mutants remained proportional to the overall SAM size, in accordance to the existence of a scaling mechanism linking meristem shape and size to *WUS* expression (Gruel et al., 2016). A similar role in meristem size regulation was already described for *FILAMENTOUS FLOWERS (FIL)* and YABBY3 (YAB3) (Goldshmidt et al., 2008). It has been suggested that the enlarged SAM in the *fil yab3* mutants results from decreased auxin synthesis in filamentous structures replacing flowers, which causes auxin depletion in the SAM and thereby increases meristem activity (Shi et al., 2018). The same mechanism could also explain the enlarged SAM observed here, that would be connected only indirectly to *LFY/RAX1* and *REV* pathways.

*RAX1 regulates a variety of pathways*

To gain insights into the molecular mechanisms controlled by RAX1, we studied RAX1 regulated genes in seedlings, unravelling links between RAX1 and proteins involved in cell wall modifications, a step know to be important for FM emergence (Armezzani et al., 2018; Tucker et al., 2018). Amongst these, we predicted that the genes encoding the cell wall modifying enzymes FUCOSYL TRANSFERASE4 (FUT4), PECTIN METHYLESTERASE3 (PME3) and EXPANSIN10 (EXPA10) and the pectin receptors WAK 1 and 2 to be likely direct targets of RAX1. All were linked to cell growth and expansion (Liang et al., 2013; Wu et al., 2010; Hewezi et al., 2008; Goh et al., 2012; Kohorn et al., 2006; Wagner and Kohorn, 2001). Additionally,

429 members of the WAK family have been linked to the regulation of cell differentiation
430 (Lally et al., 2001).

431 This analysis also revealed a role of *RAX1* in inhibiting plant defence response. This
432 seems to be a common feature of floral regulators as it is also observed for the genes
433 *LFY* and *ANT/AIL6* (Winter et al., 2011; Krizek et al., 2016). Consistently, we
434 predicted the ethylene receptors ERF1 and 2 as being direct RAX1 targets. The
435 ERFs can induce both abiotic and biotic defence pathways in response to a variety of
436 stresses (Cheng et al., 2013). Interestingly, we also detected a role of RAX1 in
437 regulating ABA and ROS responses which can also be linked to cell differentiation in
438 the SAM (Wilson et al., 2016). In particular, the ABA response regulator ABF2
439 (previously proposed to be regulated by RAX1 (Yu et al., 2016)) and the ROS
440 homeostasis regulator UPB1 are predicted direct RAX1 targets. UPB1 was shown to
441 regulate the balance of cell proliferation and differentiation in the growing root *via*
442 control of ROS homeostasis (Tsukagoshi et al., 2010). More recently, UPB1 and
443 ROS levels were shown to regulate *WUS* expression in the SAM (Zeng et al., 2017).
444 Surprisingly, we did not detect any enrichment in *CUC2* transcripts upon RAX1
445 induction. *CUC2* was shown to be a direct target of RAX1 (Tian et al., 2014).
446 However, *CUC2* is a target for microRNA degradation and therefore its ectopic
447 accumulation in the tissues used for this analysis may be prevented (Laufs et al.,
448 2004).

449 The transcriptome analysis yielded a low overlap of targets between RAX1 and REV
450 (Reinhart et al., 2013), with none clearly related to meristem homeostasis
451 (Supplemental Table 3). Despite differences in the age and growth conditions of the
452 samples between these two datasets, it suggests that RAX1 and REV act in different
453 pathways that can compensate for each other.

454 *RAX1 regulates CLV1 expression*

455 Arguably one of the most interesting targets of RAX1 in the FM homeostasis context
456 is the plasma membrane receptor CLV1, which acts as a negative regulator of *WUS*,
457 restricting the size of the OC (Lenhard and Laux, 2003). We confirmed that RAX1
458 was able to bind *in vitro* to an element from *CLV1* cis-regulatory region. Additionally,
459 induction of RAX1 activity led to a decrease in *CLV1* transcripts in inflorescences,
460 even in the presence of the protein synthesis inhibitor cycloheximide. Altogether our

data indicate that *RAX1* most likely directly regulates *CLV1* in inflorescences, providing a direct mechanistic link between *RAX1* and the regulation of meristem activity. It was shown that *WUS*-mediated repression of *CLV1* fine-tunes its expression, promoting the adaptation of the *CLV3/WUS* equilibrium (Busch et al., 2010). A similar mechanism might be leveraged by RAX1, prior to the establishment of the meristem. Fine-tuning of *CLV1* expression during FM emergence would participate to establish the new stem cell niche and the balance of *CLV3* and *WUS*, and thus define the different meristematic domains. Failure to do so would not allow a self-maintaining meristem to emerge and lead to developmental arrest, as observed in the *rax1 rev* double mutants.

This work yielded two apparently contradictory observations: both weak *rax1 rev* mutants and RAX1 over-expressers are characterized by ectopic *WUS* expression in the L1. However, we think they can be reconciled by the fact that RAX1 represses *CLV1* expression. When ectopically inducing RAX1 activity in pre-existing flower meristems, CLV1 inhibition allows the invasive expression of *WUS* throughout the flower. In the *rax1 rev* double mutants, lack of RAX1 at the very early stages of primordium formation (stage 1) would lead to a perturbation of the CLV pathway, a likely cause for a slightly decreased *WUS* expression, a shift upwards of the OC and an overall loss of meristem organization.

Recent publications showed that REV and other members of the HD-ZIPIII family directly regulate stem cell niche formation by (1) inducing STM expression, which was shown to potentiate stemness partly through activation of CK signalling (Zhang et al., 2018; Jasinski et al., 2005; Yanai et al., 2005), and (2) binding to the *WUS* promoter in a complex with B-type ARRs (Zhang et al., 2017a, 2017b). Therefore, we propose that REV and the LFY/RAX1 module control two synergistic pathways controlling the establishment of a self-sustaining floral stem-cell niche.

Our work shows that the LFY and REV pathways are essential to establish *WUS* and *CLV3* expression in floral meristems. How these regulators can be integrated into the recently proposed model where the floral stem cell niche arise from L1 signals controlling *WUS* and *CLV3* expression is not straightforward (Gruel et al., 2016). Since there is no evidence that LFY/RAX1 or REV act downstream of the L1 signals, we can imagine that they are required to regulate *WUS* level in parallel of the L1 signals. Still, the extension of WUS signal in L1 layer in some mutant combinations

we generated also suggests a more direct involvement in the action of L1 signal inhibiting WUS.

*Evolutionary perspective*

Whereas LFY was initially described for its role during flower development, it is becoming clearer that LFY ancestral role was to control cell division and apical growth (Moyroud et al., 2010; Tanahashi et al., 2005). This role is essential in the moss *Physcomitrella patens* sporophyte first divisions (Tanahashi et al., 2005) and the fern *Ceratopteris* gametophyte and sporophyte apical cells (Plackett et al., 2018). As evolution proceeded, LFY could have been co-opted as a flower regulator with the meristematic function becoming more redundant and cryptic in species such as Arabidopsis but still obvious in SAM (Zhao et al., 2018; Ahearn et al., 2001), leaves (Hofer et al., 1997; Wang et al., 2008) and axillary shoot (Rao et al., 2008) of some species. Because of its trajectory, it is likely that LEAFY has been interacting with meristematic regulator very early in evolution. Its double role is probably an efficient way to synchronize growth and identity of floral meristems. It will be interesting in the future to establish whether the LFY-RAX1 module at work in Arabidopsis flowers also plays a role in other angiosperms LEAFY related process and to determine the time of origin of the LFY-RAX1 module.

## Experimental Procedures

*Plant material and treatments*

The *rax1-3, rev-6*, and *lfy-12* alleles have been previously described (Müller et al., 2006; Weigel et al., 1992; Otsuga et al., 2001). *rev-6* mutants (L*er*) and *rax1-3* mutants (Col) were crossed and the double mutants were backcrossed 3 times to Col. Further work was performed on the progeny of the backcrossed plants. Plants were cultivated in long-day conditions (16h light) unless specified otherwise. The *pLFY:LFY-VP16* line was previously described (Parcy et al., 1998). For confocal and scanning electron microscopy, plants were grown in short-day conditions (8 h of light) for 6 weeks and transferred to long-day conditions for 2 weeks. Mutants phenotyping was performed three weeks after bolting. For DEX treatment the plants were sprayed

with either 10 µM DEX in 1/10 000 DMSO or ethanol or 1/10 000 DMSO or ethanol (mock) every other day from two weeks on.

*Reporter constructs*

The *pRAX1:GUS* construct contains 2.1 kb of *RAX1* promoter driving GUS expression. The *pWUS:Venus* construct was generated by combining pGGA003, pGGB002, 2xVenus, pGGD007, pGGE002 and pGGF003 in PGGZ001 in a single step GreenGate reaction (Lampropoulos et al., 2013). All constructs were transformed by the floral dip method (Logemann et al., 2006), several independent lines were analysed and a representative one was selected for further work.

*CRISPR constructs*

CRISPR spacers were designed using CHOPCHOP (Montague et al., 2014). Spacers with no predicted off-targets were selected (Supplemental Table 4). Spacers were cloned in pAtU6-26-v4, *pAtU6-26:gRNA* and *pUBQ10:Cas9:tNOS* expression cassettes were then combined in pCAMBIA1300 (Yan et al., 2016).

*RAX1 inducible constructs*

*RAX1* cDNA in pDONR221 (DQ446976) was acquired from ABRC. The internal *Bsa*I site was removed by mutagenesis using oGD122 and oGD123 (Supplemental Table 5). The sequence was subsequently amplified with oGD115 and oGD116, which added the compatible GreenGate overhangs and flanking *Bsa*I sites, and was cloned in pGGC000, producing pGD41. The GR coding sequence was amplified from plants carrying an APETALA1-GR construct (Wellmer et al., 2006) with oGD109 and oGD110 to be cloned in pGGC000 to produce pGD38. For the cloning of GR in pGGD000, a linker sequence was amplified from pGGD001 with oGD118 and oGD119 and the GR sequence was amplified with oGD110 and oGD111. Both fragments were cloned with compatible ends in pGGD000 in a single step ligation to produce pGD39. The Alligator selection cassette (At2S3:GFP) was amplified from pALLIGATOR1 (Bensmihen et al., 2004) with oGD120 and oGD121 and cloned in pGGF000 to produce pGD43. The construct *pUBQ10:mCHERRY-RAX1-GR:tUBQ10:Alligator* (iRAX1) was produced in a single step GreenGate reaction with the plasmids pGGZ001, pGGA006, pGGE009, pGD43, pGGB001, pGD41 and pGD39. The construct *pUBQ10:mCHERRY-GR-NLS:tUBQ10:Alligator* (iMock) was

555 produced with the plasmids pGGZ001, pGGA006, pGGE009, pGGB001, pGD38 and
556 pGD002. Constructs were transformed in Arabidopsis by the floral dip method
557 (Logemann et al., 2006) and T1 plants were selected based on seed fluorescence.
558 Several independent lines were analysed in the T2 generation for mCherry
559 translocation in the nuclei and phenotypical effects upon DEX treatment. A single line
560 was selected for further analysis.

561 *RAX1 constructs for in vitro expression*

562 The internal *Nco*I site in RAX1 cDNA was removed by mutagenesis with oGD03 and
563 oGD04. The resulting sequence was amplified with oGD01 and oGD02 for the
564 cloning of the full-length sequence and oGD01 and oGD05 for the cloning of the Myb
565 domain. The latter primers added *Nco*I and *Not*I restriction sites which were used to
566 transfer the amplicon to the destination plasmid. The full length cDNA was
567 transferred to pETM41 (Dümmler et al., 2005), which contains the sequence for an
568 6xHis tag and an MBP tag, producing pGD19. The sequence corresponding to the
569 Myb domain was transferred to pETM11 (Dümmler et al., 2005), which contains the
570 sequence for a 6xHis tag, producing pGD14.

571 *Identification and isolation of CRISPR mutants*

572 CRISPR constructs were transformed in *pWUS:VENUS* background by the floral dip
573 method (Logemann et al., 2006). Several T1 plants were selected based on
574 Hygromycin resistance. CRISPR-induced mutations were identified in the T2 using
575 poly-acrylamide gel electrophoresis (PAGE) separation of DNA heteroduplexes (Zhu
576 et al., 2014). The regions surrounding RAX1 spacers 1 and 2 were amplified with
577 oGD124 and oGD126, and oGD125 and oGD134 respectively. The regions
578 surrounding REV spacers 1 and 2 were amplified with oGD127 and oGD129, and
579 oGD128 and oGD135 respectively. These regions were subcloned in pCR-Blunt
580 (ThermoFisher) for sequencing. Selected lines for the single mutants in either *RAX1*
581 or *REV* carried a homozygous mutation (namely *rax1-c1* and *rev-c1*), however the
582 double mutant line carried heteroallelic mutations at each locus (*rax1-c2/c3 rev-*
583 *c2/*c3; see Figure S1). Progeny of these plants was used for further characterization.
584 CRISPR lines targeting *REV* were crossed to *lfy-12* and T2 was screened for double
585 mutant genotype. A line carrying homozygous mutation at the *REV* loci (*rev-c4*) and
586 heterozygous *lfy-12* mutation was selected.

587 *Western blotting*

588 mCHERRY expression was detected in seedlings whole extract using the [6G6] anti-
589 RFP antibody (ChromoTek) at a dilution of 1/1000 and revealed with HRP-coupled
590 anti-mouse antibody. Western blotting was performed as described previously
591 (Sayou et al., 2016).

592 *In situ hybridization*

593 Plant samples were harvested shortly after bolting. Older flowers were swiftly
594 removed, apices were collected in fixative, and *in situ* hybridization was performed as
595 previously described (Carles et al., 2010). The *RAX1, WUS,* and *CLV3* probes were
596 described in previous studies (Fletcher et al., 1999; Brand et al., 2000; Keller et al.,
597 2006).

598 *Scanning electron microscopy*

599 Older flowers were removed from the inflorescences. Apices were collected and
600 swiftly fixed on a stub by carbon tape. A drop of water was added at the base of the
601 inflorescence and the samples were placed in the FEI Quanta 250 chamber. Imaging
602 was performed in ESEM mode with a pressure between 700 and 550 Pa and a
603 temperature of 1°C to 2°C with a tension of 14 kV.

604 *Confocal microscopy and image treatment*

605 Apices were dissected and placed on 2% agarose and cell walls were counter-
606 stained with FM4-64 or propidium iodide. Cell wall and VENUS signals were recorded
607 in two separate channels. Imaging was performed on a Zeiss 780 (for the *lfy rev*
608 mutants) or a Leica SP2 (for the *rax1 rev* mutants) with a 40X Water immersion long-
609 distance objective. Image treatment was performed with FIJI (Schindelin et al., 2012).
610 Minimal and maximal values were set to improve signal-to-noise ratio, and are
611 indicated next to the images. For dexamethasone (DEX) induction, the apices were
612 placed on apex culture medium (Hamant et al., 2014) containing 1/10 000 DMSO or
613 ethanol with or without 10 µM DEX. Samples were imaged after 6-24 h of incubation.

614 *RNA sequencing and analysis*

615 14-day-old seedlings grown on MS plates were shortly immersed with a solution
616 containing 0.03% L-77 Silwett and 1/10 000 DMSO (mock), or 10 µM DEX (DEX).

Whole seedlings were harvested 4 h after treatment and immediately flash-frozen in liquid nitrogen. RNA was extracted with the RNAeasy kit (Qiagen) and DNA was removed with the TURBO DNA-free kit (Ambion) according to manufacturer's instructions. Libraries were synthesized with the TruSeq Stranded kit (Illumina) and paired-end sequencing was performed on an HiSeq2000 (Illumina) at the POPS platform (IPS2, Paris-Saclay). Adapter sequences were trimmed and duplicated and low-quality reads were discarded. Mapping was performed on TAIR10 assembly with HISAT2 (Kim et al., 2015) and mapped reads with a mapping quality score below 30 or mapped at several locations were discarded, resulting in an average of 97% of uniquely mapped read pairs. Reads mapped to exons or untranslated regions were counted with HTSeq (Anders et al., 2015). DEG discovery was performed with EdgeR (Robinson et al., 2010) using a multiparametric GLM model for the interaction genotype:treatment after TMM normalization (McCarthy et al., 2012; Zhou et al., 2014; Robinson and Smyth, 2007). Genes were considered differentially expressed if the likelihood-ratio test FDR was equal or below 0.01. GO-term enrichment analysis was performed in Araport (Krishnakumar et al., 2015).

*RAX1 binding-site prediction*

PBM was performed as previously described using an MBP tagged full-length RAX1 fusion protein (Franco-Zorrilla and Solano, 2014). Binding sites were predicted using the Biopython package for python 2.7 (Cock et al., 2009). pOcc was calculated as described for the GOMER program (Granek and Clarke, 2005). All analyses were performed on the extended genomic sequence spanning 3 kb upstream to 3 kb downstream of transcribed regions.

*qRT-PCR*

Shortly after bolting, inflorescences were treated with a drop of solution containing 0.03% L-77 Silwett, 1/10 000 DMSO, and 1/1 000 ethanol (mock), and alternatively 10 µM DEX (DEX), 50 µM cycloheximide (CHX) or both (DEX+CHX). Older flowers were dissected and 6 inflorescences per replicate were harvested. RNA was extracted with the RNAeasy kit (Qiagen). Gene expression was quantified using AT2G28390 and AT4G34270 as internal reference as they were shown to be stable across a wide range of conditions (Czechowski et al., 2005). Statistical analysis was

performed on the ΔCq values and fold-change was calculated solely for graphical representation purpose.

*In vitro DNA-binding assay*

Protein production was performed as previously described (Sayou et al., 2016). Proteins were purified on nickel-sepharose column in purification buffer (Tris-HCl 20mM; dithiothreitol 1mM; pH7.5) and eluted with 150mM imidazole before dialysis in purification buffer. Electrophoretic mobility-shift assay was performed as previously described (Sayou et al., 2016) in binding buffer (Tris-HCl 10 mM; NaCl 50 mM; $MgCl_2$ 1 mM; 1% glycerol; EDTA 0.5 mM; DTT 1 mM; pH 7.5). Probe sequences are indicated in Supplemental Table 6.

## Accessions

RNA sequencing raw and processed files are available from ArrayExpress (E-MTAB-7050).

## Supplementary Data

Supplemental Figure 1. CRISPR/Cas9-induced mutations in *REV* and *RAX1*.
Supplemental Figure 2. Characterization of the *WUS* transcriptional reporter expression in flower primordia.
Supplemental Figure 3. Phenotypic characterization of the *rax1, rev* and *rax1 rev* CRISPR lines.
Supplemental Figure 4. Expression of *WUS* in the *rev-c4* and *lfy-12 rev-c4* mutants.
Supplemental Figure 5. LFY induces *RAX1* expression in inflorescences.
Supplemental Figure 6. Growth habit of *rax1-3, rev-6* and double mutant in long-day inductive conditions.
Supplemental Figure 7. Axillary organ formation in *rax1-3 rev-6* F2 population.
Supplemental Figure 8. *rax1-3* and *rev-6* mutant phenotype in non-inductive short-day conditions.
Supplemental Figure 9. Abnormal flower primordia in *rax1 rev* lack detectable *WUS* and *CLV3* transcripts.
Supplemental Figure 10. Enlarged shoot apical meristems in the *rax1 rev* mutants.
Supplemental Figure 11. Effects of RAX1 activity induction on growth and development.

679 Supplemental Table 1. Segregation analysis of *lfy-12* and *rev-c4* mutations.
680 Supplemental Table 2. Non exhaustive list of predicted putative direct RAX1 targets.
681 Supplemental Table 3. Genes co-regulated by RAX1 and REV.
682 Supplemental Table 4. CRISPR spacers sequences.
683 Supplemental Table 5. Primers used in this study.
684 Supplemental Table 6. EMSA probes used in this study.
685 Supplementary Dataset 1: List of DEG in response to RAX1 induction
686 Supplementary Dataset 2: GO term enrichment in DEG
687 Supplementary Dataset 3: Gene-sorted GO term enrichment
688 Supplementary Dataset 4: RAX1 best binding score and predicted occupancy in DEG
689 promoter regions.

690 **Author Contributions**

691 DG, TG and PF conceived and design the work. DG, TG, LMM, CH, HS, and LVI
692 collected and analysed data. WC, FZJM, SR and LJ provided material and/or
693 expertise essential for this work.

694 **Acknowledgments**

695 The authors wish to acknowledge the support of the Electron Microscopy facility of
696 the ICMG Nanobio – Chemistry Platform and C. Lancelon-Pin in particular. The
697 POPS transcriptomic platform and L. Soubignou-Taconnat. S. Figuet and D.
698 Grunwald for shared facilities. K. Kaufmann and W. Yan for sharing plasmids ahead
699 of publication, E. Delannoy, M-L. Martin-Magniette, P. Das, L. Comai and A. Larrieu
700 for their inputs on the project. pRAX1:GUS seeds were a generous gift from P.
701 Doerner. This work was supported by the French National Agency for Research
702 programs Charmful (ANRBlanc–SVSE2– 2011) and Gral (ANR-10-LABX-49-01). The
703 platform POPS benefits from the support of the LabEx Saclay Plant Sciences-SPS
704 (ANR-10-LABX-0040-SPS).

705 **References**

706 **Ahearn, K.P., Johnson, H.A., Weigel, D., and Wagner, D.R.** (2001). NFL1, a Nicotiana
707 tabacum LEAFY-like gene, controls meristem initiation and floral structure. Plant Cell
708 Physiol **42**: 1130–1139.

709 **Anders, S., Pyl, P.T., and Huber, W.** (2015). HTSeq — a Python framework to work with
710 high-throughput sequencing data. Bioinformatics **31**: 166–169.

**Armezzani, A. et al.** (2018). Transcriptional induction of cell wall remodelling genes is coupled to microtubule-driven growth isotropy at the shoot apex in Arabidopsis. Development **145**.

**Bensmihen, S., To, A., Lambert, G., Kroj, T., Giraudat, J., and Parcy, F.** (2004). Analysis of an activated ABI5 allele using a new selection method for transgenic Arabidopsis seeds. FEBS Lett **561**: 127–131.

**Blázquez, M.A., Soowal, L.N., Lee, I., and Weigel, D.** (1997). LEAFY expression and flower initiation in Arabidopsis. Development **124**: 3835–3844.

**Brand, U., Fletcher, J.C., Hobe, M., Meyerowitz, E.M., and Simon, R.** (2000). Dependence of stem cell fate in Arabidopsis on a feedback loop regulated by CLV3 activity. Science **289**: 617–619.

**Brand, U., Grünewald, M., Hobe, M., and Simon, R.** (2002). Regulation of CLV3 expression by two homeobox genes in Arabidopsis. Plant Physiol **129**: 565–575.

**Busch, W. et al.** (2010). Transcriptional control of a plant stem cell niche. Dev Cell **18**: 849–861.

**Caggiano, M.P., Yu, X., Bhatia, N., Larsson, A., Ram, H., Ohno, C.K., Sappl, P., Meyerowitz, E.M., Jönsson, H., and Heisler, M.G.** (2017). Cell type boundaries organize plant development. elife **6**.

**Carles, C.C., Ha, C.M., Jun, J.H., Fiume, E., and Fletcher, J.C.** (2010). Analyzing shoot apical meristem development. Methods Mol Biol **655**: 105–129.

**Chahtane, H. et al.** (2013). A variant of LEAFY reveals its capacity to stimulate meristem development by inducing RAX1. Plant J **74**: 678–689.

**Chahtane, H., Zhang, B., Norberg, M., LeMasson, M., Thévenon, E., Bakó, L., Benlloch, R., Holmlund, M., Parcy, F., Nilsson, O., and Vachon, G.** (2018). LEAFY activity is post-transcriptionally regulated by BLADE ON PETIOLE2 and CULLIN3 in Arabidopsis. New Phytol **220**: 579–592.

**Chandler, J.W. and Werr, W.** (2014). Arabidopsis floral phytomer development: auxin response relative to biphasic modes of organ initiation. J Exp Bot **65**: 3097–3110.

**Cheng, M.-C., Liao, P.-M., Kuo, W.-W., and Lin, T.-P.** (2013). The Arabidopsis ETHYLENE RESPONSE FACTOR1 regulates abiotic stress-responsive gene expression by binding to different cis-acting elements in response to different stress signals. Plant Physiol **162**: 1566–1582.

**Cock, P.J.A., Antao, T., Chang, J.T., Chapman, B.A., Cox, C.J., Dalke, A., Friedberg, I., Hamelryck, T., Kauff, F., Wilczynski, B., and de Hoon, M.J.L.** (2009). Biopython: freely available Python tools for computational molecular biology and bioinformatics. Bioinformatics **25**: 1422–1423.

**Czechowski, T., Stitt, M., Altmann, T., Udvardi, M.K., and Scheible, W.-R.** (2005). Genome-wide identification and testing of superior reference genes for transcript normalization in Arabidopsis. Plant Physiol **139**: 5–17.

**Denay, G., Chahtane, H., Tichtinsky, G., and Parcy, F.** (2017). A flower is born: an updateon Arabidopsis floral meristem formation. Curr Opin Plant Biol.

752 **Dümmler, A., Lawrence, A.-M., and de Marco, A.** (2005). Simplified screening for the
753 detection of soluble fusion constructs expressed in E. coli using a modular set of
754 vectors. Microb Cell Fact **4**: 34.

755 **Endrizzi, K., Moussian, B., Haecker, A., Levin, J.Z., and Laux, T.** (1996). The SHOOT
756 MERISTEMLESS gene is required for maintenance of undifferentiated cells in
757 Arabidopsis shoot and floral meristems and acts at a different regulatory level than
758 the meristem genes WUSCHEL and ZWILLE. Plant J **10**: 967–979.

759 **Fletcher, J.C., Brand, U., Running, M.P., Simon, R., and Meyerowitz, E.M.** (1999).
760 Signaling of cell fate decisions by CLAVATA3 in Arabidopsis shoot meristems.
761 Science **283**: 1911–1914.

762 **Franco-Zorrilla, J.M., López-Vidriero, I., Carrasco, J.L., Godoy, M., Vera, P., and Solano,**
763 **R.** (2014). DNA-binding specificities of plant transcription factors and their potential to
764 define target genes. Proc Natl Acad Sci U S A **111**: 2367–2372.

765 **Franco-Zorrilla, J.M. and Solano, R.** (2014). High-throughput analysis of protein-DNA
766 binding affinity. Methods Mol Biol **1062**: 697–709.

767 **Gaillochet, C., Daum, G., and Lohmann, J.U.** (2015). O cell, where art thou? The
768 mechanisms of shoot meristem patterning. Curr Opin Plant Biol **23**: 91–97.

769 **Geldner, N., Dénervaud-Tendon, V., Hyman, D.L., Mayer, U., Stierhof, Y.-D., and Chory,**
770 **J.** (2009). Rapid, combinatorial analysis of membrane compartments in intact plants
771 with a multicolor marker set. Plant J **59**: 169–178.

772 **Goh, H.-H., Sloan, J., Dorca-Fornell, C., and Fleming, A.** (2012). Inducible repression of
773 multiple expansin genes leads to growth suppression during leaf development. Plant
774 Physiol **159**: 1759–1770.

775 **Goldshmidt, A., Alvarez, J.P., Bowman, J.L., and Eshed, Y.** (2008). Signals derived from
776 YABBY gene activities in organ primordia regulate growth and partitioning of
777 Arabidopsis shoot apical meristems. Plant Cell **20**: 1217–1230.

778 **Gordon, S.P., Chickarmane, V.S., Ohno, C., and Meyerowitz, E.M.** (2009). Multiple
779 feedback loops through cytokinin signaling control stem cell number within the
780 Arabidopsis shoot meristem. Proc Natl Acad Sci U S A **106**: 16529–16534.

781 **Granek, J.A. and Clarke, N.D.** (2005). Explicit equilibrium modeling of transcription-factor
782 binding and gene regulation. Genome Biol **6**: R87.

783 **Gruel, J., Landrein, B., Tarr, P., Schuster, C., Refahi, Y., Sampathkumar, A., Hamant,**
784 **O., Meyerowitz, E.M., and Jönsson, H.** (2016). An epidermis-driven mechanism
785 positions and scales stem cell niches in plants. Science advances **2**: e1500989.

786 **Guo, D., Zhang, J., Wang, X., Han, X., Wei, B., Wang, J., Li, B., Yu, H., Huang, Q., Gu, H.,**
787 **Qu, L.-J., and Qin, G.** (2015). The WRKY transcription factor WRKY71/EXB1
788 controls shoot branching by transcriptionally regulating RAX genes in arabidopsis.
789 Plant Cell **27**: 3112–3127.

790 **Hamant, O., Das, P., and Burian, A.** (2014). Time-lapse imaging of developing meristems
791 using confocal laser scanning microscope. Methods Mol Biol **1080**: 111–119.

792 **Hewezi, T., Howe, P., Maier, T.R., Hussey, R.S., Mitchum, M.G., Davis, E.L., and Baum,**
793 **T.J.** (2008). Cellulose binding protein from the parasitic nematode Heterodera

794 schachtii interacts with Arabidopsis pectin methylesterase: cooperative cell wall
795 modification during parasitism. Plant Cell **20**: 3080–3093.

796 **Hofer, J., Turner, L., Hellens, R., Ambrose, M., Matthews, P., Michael, A., and Ellis, N.**
797 (1997). UNIFOLIATA regulates leaf and flower morphogenesis in pea. Curr Biol **7**:
798 581–587.

799 **Hwang, I. and Sheen, J.** (2001). Two-component circuitry in Arabidopsis cytokinin signal
800 transduction. Nature **413**: 383–389.

801 **Jasinski, S., Piazza, P., Craft, J., Hay, A., Woolley, L., Rieu, I., Phillips, A., Hedden, P.,**
802 **and Tsiantis, M.** (2005). KNOX action in Arabidopsis is mediated by coordinate
803 regulation of cytokinin and gibberellin activities. Curr Biol **15**: 1560–1565.

804 **Kaufmann, K., Wellmer, F., Muiño, J.M., Ferrier, T., Wuest, S.E., Kumar, V., Serrano-**
805 **Mislata, A., Madueño, F., Krajewski, P., Meyerowitz, E.M., Angenent, G.C., and**
806 **Riechmann, J.L.** (2010). Orchestration of floral initiation by APETALA1. Science **328**:
807 85–89.

808 **Keller, T., Abbott, J., Moritz, T., and Doerner, P.** (2006). Arabidopsis REGULATOR OF
809 AXILLARY MERISTEMS1 controls a leaf axil stem cell niche and modulates
810 vegetative development. Plant Cell **18**: 598–611.

811 **Kim, D., Langmead, B., and Salzberg, S.L.** (2015). HISAT: a fast spliced aligner with low
812 memory requirements. Nat Methods **12**: 357–360.

813 **Kim, S., Kang, J.-Y., Cho, D.-I., Park, J.H., and Kim, S.Y.** (2004). ABF2, an ABRE-binding
814 bZIP factor, is an essential component of glucose signaling and its overexpression
815 affects multiple stress tolerance. Plant J **40**: 75–87.

816 **Kohorn, B.D., Kobayashi, M., Johansen, S., Riese, J., Huang, L.-F., Koch, K., Fu, S.,**
817 **Dotson, A., and Byers, N.** (2006). An Arabidopsis cell wall-associated kinase
818 required for invertase activity and cell growth. Plant J **46**: 307–316.

819 **Krishnakumar, V. et al.** (2015). Araport: the Arabidopsis information portal. Nucleic Acids
820 Res **43**: D1003–9.

821 **Krizek, B.A., Bequette, C.J., Xu, K., Blakley, I.C., Fu, Z.Q., Stratmann, J., and Loraine,**
822 **A.E.** (2016). RNA-Seq links AINTEGUMENTA and AINTEGUMENTA-LIKE6 to cell
823 wall remodeling and plant defense pathways in Arabidopsis. Plant Physiol **171**: 2069–
824 2084.

825 **Lally, D., Ingmire, P., Tong, H.Y., and He, Z.H.** (2001). Antisense expression of a cell wall-
826 associated protein kinase, WAK4, inhibits cell elongation and alters morphology.
827 Plant Cell **13**: 1317–1331.

828 **Lampropoulos, A., Sutikovic, Z., Wenzl, C., Maegele, I., Lohmann, J.U., and Forner, J.**
829 (2013). GreenGate---a novel, versatile, and efficient cloning system for plant
830 transgenesis. PLoS ONE **8**: e83043.

831 **Laufs, P., Peaucelle, A., Morin, H., and Traas, J.** (2004). MicroRNA regulation of the CUC
832 genes is required for boundary size control in Arabidopsis meristems. Development
833 **131**: 4311–4322.

834 **Laux, T., Mayer, K.F., Berger, J., and Jürgens, G.** (1996). The WUSCHEL gene is required
835 for shoot and floral meristem integrity in Arabidopsis. Development **122**: 87–96.

**Leibfried, A., To, J.P.C., Busch, W., Stehling, S., Kehle, A., Demar, M., Kieber, J.J., and Lohmann, J.U.** (2005). WUSCHEL controls meristem function by direct regulation of cytokinin-inducible response regulators. Nature **438**: 1172–1175.

**Lenhard, M., Jürgens, G., and Laux, T.** (2002). The WUSCHEL and SHOOTMERISTEMLESS genes fulfil complementary roles in Arabidopsis shoot meristem regulation. Development **129**: 3195–3206.

**Lenhard, M. and Laux, T.** (2003). Stem cell homeostasis in the Arabidopsis shoot meristem is regulated by intercellular movement of CLAVATA3 and its sequestration by CLAVATA1. Development **130**: 3163–3173.

**Liang, Y., Basu, D., Pattathil, S., Xu, W.-L., Venetos, A., Martin, S.L., Faik, A., Hahn, M.G., and Showalter, A.M.** (2013). Biochemical and physiological characterization of fut4 and fut6 mutants defective in arabinogalactan-protein fucosylation in Arabidopsis. J Exp Bot **64**: 5537–5551.

**Logemann, E., Birkenbihl, R.P., Ulker, B., and Somssich, I.E.** (2006). An improved method for preparing Agrobacterium cells that simplifies the Arabidopsis transformation protocol. Plant Methods **2**: 16.

**Lohmann, J.U., Hong, R.L., Hobe, M., Busch, M.A., Parcy, F., Simon, R., and Weigel, D.** (2001). A molecular link between stem cell regulation and floral patterning in Arabidopsis. Cell **105**: 793–803.

**Mayer, K.F., Schoof, H., Haecker, A., Lenhard, M., Jürgens, G., and Laux, T.** (1998). Role of WUSCHEL in regulating stem cell fate in the Arabidopsis shoot meristem. Cell **95**: 805–815.

**McCarthy, D.J., Chen, Y., and Smyth, G.K.** (2012). Differential expression analysis of multifactor RNA-Seq experiments with respect to biological variation. Nucleic Acids Res **40**: 4288–4297.

**Montague, T.G., Cruz, J.M., Gagnon, J.A., Church, G.M., and Valen, E.** (2014). CHOPCHOP: a CRISPR/Cas9 and TALEN web tool for genome editing. Nucleic Acids Res **42**: W401–7.

**Moyroud, E., Kusters, E., Monniaux, M., Koes, R., and Parcy, F.** (2010). LEAFY blossoms. Trends Plant Sci **15**: 346–352.

**Moyroud, E., Minguet, E.G., Ott, F., Yant, L., Posé, D., Monniaux, M., Blanchet, S., Bastien, O., Thévenon, E., Weigel, D., Schmid, M., and Parcy, F.** (2011). Prediction of regulatory interactions from genome sequences using a biophysical model for the Arabidopsis LEAFY transcription factor. Plant Cell **23**: 1293–1306.

**Müller, D., Schmitz, G., and Theres, K.** (2006). Blind homologous R2R3 Myb genes control the pattern of lateral meristem initiation in Arabidopsis. Plant Cell **18**: 586–597.

**Ogawa, M., Shinohara, H., Sakagami, Y., and Matsubayashi, Y.** (2008). Arabidopsis CLV3 peptide directly binds CLV1 ectodomain. Science **319**: 294.

**Otsuga, D., DeGuzman, B., Prigge, M.J., Drews, G.N., and Clark, S.E.** (2001). REVOLUTA regulates meristem initiation at lateral positions. Plant J **25**: 223–236.

**Padidam, M.** (2003). Chemically regulated gene expression in plants. Curr Opin Plant Biol **6**: 169–177.

878 **Parcy, F., Nilsson, O., Busch, M.A., Lee, I., and Weigel, D.** (1998). A genetic framework
879 for floral patterning. Nature **395**: 561–566.

880 **Plackett, A.R., Conway, S.J., Hewett Hazelton, K.D., Rabbinowitsch, E.H., Langdale,**
881 **J.A., and Di Stilio, V.S.** (2018). LEAFY maintains apical stem cell activity during
882 shoot development in the fern Ceratopteris richardii. elife **7**.

883 **Prigge, M.J., Otsuga, D., Alonso, J.M., Ecker, J.R., Drews, G.N., and Clark, S.E.** (2005).
884 Class III homeodomain-leucine zipper gene family members have overlapping,
885 antagonistic, and distinct roles in Arabidopsis development. Plant Cell **17**: 61–76.

886 **Rao, N.N., Prasad, K., Kumar, P.R., and Vijayraghavan, U.** (2008). Distinct regulatory role
887 for RFL, the rice LFY homolog, in determining flowering time and plant architecture.
888 Proc Natl Acad Sci U S A **105**: 3646–3651.

889 **Reinhart, B.J., Liu, T., Newell, N.R., Magnani, E., Huang, T., Kerstetter, R., Michaels, S.,**
890 **and Barton, M.K.** (2013). Establishing a framework for the Ad/abaxial regulatory
891 network of Arabidopsis: ascertaining targets of class III homeodomain leucine zipper
892 and KANADI regulation. Plant Cell **25**: 3228–3249.

893 **Robinson, M.D., McCarthy, D.J., and Smyth, G.K.** (2010). edgeR: a Bioconductor package
894 for differential expression analysis of digital gene expression data. Bioinformatics **26**:
895 139–140.

896 **Robinson, M.D. and Smyth, G.K.** (2007). Moderated statistical tests for assessing
897 differences in tag abundance. Bioinformatics **23**: 2881–2887.

898 **Sakai, H., Honma, T., Aoyama, T., Sato, S., Kato, T., Tabata, S., and Oka, A.** (2001).
899 ARR1, a transcription factor for genes immediately responsive to cytokinins. Science
900 **294**: 1519–1521.

901 **Samach, A., Klenz, J.E., Kohalmi, S.E., Risseeuw, E., Haughn, G.W., and Crosby, W.L.**
902 (1999). The UNUSUAL FLORAL ORGANS gene of Arabidopsis thaliana is an F-box
903 protein required for normal patterning and growth in the floral meristem. Plant J **20**:
904 433–445.

905 **Sawa, S., Ito, T., Shimura, Y., and Okada, K.** (1999). FILAMENTOUS FLOWER controls
906 the formation and development of arabidopsis inflorescences and floral meristems.
907 Plant Cell **11**: 69–86.

908 **Sayou, C. et al.** (2016). A SAM oligomerization domain shapes the genomic binding
909 landscape of the LEAFY transcription factor. Nat Commun **7**: 11222.

910 **Schindelin, J. et al.** (2012). Fiji: an open-source platform for biological-image analysis. Nat
911 Methods **9**: 676–682.

912 **Schoof, H., Lenhard, M., Haecker, A., Mayer, K.F., Jürgens, G., and Laux, T.** (2000). The
913 stem cell population of Arabidopsis shoot meristems in maintained by a regulatory
914 loop between the CLAVATA and WUSCHEL genes. Cell **100**: 635–644.

915 **Shi, B. et al.** (2016). Two-Step Regulation of a Meristematic Cell Population Acting in Shoot
916 Branching in Arabidopsis. PLoS Genet **12**: e1006168.

917 **Shi, B., Guo, X., Wang, Y., Xiong, Y., Wang, J., Hayashi, K.-I., Lei, J., Zhang, L., and**
918 **Jiao, Y.** (2018). Feedback from Lateral Organs Controls Shoot Apical Meristem
919 Growth by Modulating Auxin Transport. Dev Cell **44**: 204–216.e6.

**Talbert, P.B., Adler, H.T., Parks, D.W., and Comai, L.** (1995). The REVOLUTA gene is necessary for apical meristem development and for limiting cell divisions in the leaves and stems of Arabidopsis thaliana. Development **121**: 2723–2735.

**Tanahashi, T., Sumikawa, N., Kato, M., and Hasebe, M.** (2005). Diversification of gene function: homologs of the floral regulator FLO/LFY control the first zygotic cell division in the moss Physcomitrella patens. Development **132**: 1727–1736.

**Tian, C. et al.** (2014). An organ boundary-enriched gene regulatory network uncovers regulatory hierarchies underlying axillary meristem initiation. Mol Syst Biol **10**: 755.

**Tsukagoshi, H., Busch, W., and Benfey, P.N.** (2010). Transcriptional regulation of ROS controls transition from proliferation to differentiation in the root. Cell **143**: 606–616.

**Tucker, M.R., Lou, H., Aubert, M.K., Wilkinson, L.G., Little, A., Houston, K., Pinto, S.C., and Shirley, N.J.** (2018). Exploring the Role of Cell Wall-Related Genes and Polysaccharides during Plant Development. Plants **7**.

**Wagner, T.A. and Kohorn, B.D.** (2001). Wall-associated kinases are expressed throughout plant development and are required for cell expansion. Plant Cell **13**: 303–318.

**Wang, H., Chen, J., Wen, J., Tadege, M., Li, G., Liu, Y., Mysore, K.S., Ratet, P., and Chen, R.** (2008). Control of compound leaf development by FLORICAULA/LEAFY ortholog SINGLE LEAFLET1 in Medicago truncatula. Plant Physiol **146**: 1759–1772.

**Weigel, D., Alvarez, J., Smyth, D.R., Yanofsky, M.F., and Meyerowitz, E.M.** (1992). LEAFY controls floral meristem identity in Arabidopsis. Cell **69**: 843–859.

**Wellmer, F., Alves-Ferreira, M., Dubois, A., Riechmann, J.L., and Meyerowitz, E.M.** (2006). Genome-wide analysis of gene expression during early Arabidopsis flower development. PLoS Genet **2**: e117.

**Wilkinson, M.D. and Haughn, G.W.** (1995). UNUSUAL FLORAL ORGANS controls meristem identity and organ primordia fate in arabidopsis. Plant Cell **7**: 1485–1499.

**Wilson, M.E., Mixdorf, M., Berg, R.H., and Haswell, E.S.** (2016). Plastid osmotic stress influences cell differentiation at the plant shoot apex. Development **143**: 3382–3393.

**Winter, C.M. et al.** (2011). LEAFY target genes reveal floral regulatory logic, cis motifs, and a link to biotic stimulus response. Dev Cell **20**: 430–443.

**Wu, M.-F., Yamaguchi, N., Xiao, J., Bargmann, B., Estelle, M., Sang, Y., and Wagner, D.** (2015). Auxin-regulated chromatin switch directs acquisition of flower primordium founder fate. elife **4**: e09269.

**Wu, Y., Williams, M., Bernard, S., Driouich, A., Showalter, A.M., and Faik, A.** (2010). Functional identification of two nonredundant Arabidopsis alpha(1,2)fucosyltransferases specific to arabinogalactan proteins. J Biol Chem **285**: 13638–13645.

**Yadav, R.K., Girke, T., Pasala, S., Xie, M., and Reddy, G.V.** (2009). Gene expression map of the Arabidopsis shoot apical meristem stem cell niche. Proc Natl Acad Sci U S A **106**: 4941–4946.

**Yadav, R.K., Perales, M., Gruel, J., Girke, T., Jönsson, H., and Reddy, G.V.** (2011). WUSCHEL protein movement mediates stem cell homeostasis in the Arabidopsis shoot apex. Genes Dev **25**: 2025–2030.

962 **Yadav, R.K., Perales, M., Gruel, J., Ohno, C., Heisler, M., Girke, T., Jönsson, H., and**
963 **Reddy, G.V.** (2013). Plant stem cell maintenance involves direct transcriptional
964 repression of differentiation program. Mol Syst Biol **9**: 654.

965 **Yadav, R.K. and Reddy, G.V.** (2012). WUSCHEL protein movement and stem cell
966 homeostasis. Plant Signal Behav **7**: 592–594.

967 **Yadav, R.K., Tavakkoli, M., and Reddy, G.V.** (2010). WUSCHEL mediates stem cell
968 homeostasis by regulating stem cell number and patterns of cell division and
969 differentiation of stem cell progenitors. Development **137**: 3581–3589.

970 **Yadav, R.K., Tavakkoli, M., Xie, M., Girke, T., and Reddy, G.V.** (2014). A high-resolution
971 gene expression map of the Arabidopsis shoot meristem stem cell niche.
972 Development **141**: 2735–2744.

973 **Yamaguchi, N., Wu, M.-F., Winter, C.M., Berns, M.C., Nole-Wilson, S., Yamaguchi, A.,**
974 **Coupland, G., Krizek, B.A., and Wagner, D.** (2013). A molecular framework for
975 auxin-mediated initiation of flower primordia. Dev Cell **24**: 271–282.

976 **Yan, W., Chen, D., and Kaufmann, K.** (2016). Efficient multiplex mutagenesis by RNA-
977 guided Cas9 and its use in the characterization of regulatory elements in the
978 AGAMOUS gene. Plant Methods **12**: 23.

979 **Yanai, O., Shani, E., Dolezal, K., Tarkowski, P., Sablowski, R., Sandberg, G., Samach,**
980 **A., and Ori, N.** (2005). Arabidopsis KNOXI proteins activate cytokinin biosynthesis.
981 Curr Biol **15**: 1566–1571.

982 **Yoshida, S., Mandel, T., and Kuhlemeier, C.** (2011). Stem cell activation by light guides
983 plant organogenesis. Genes Dev **25**: 1439–1450.

984 **Yu, Y.-T., Wu, Z., Lu, K., Bi, C., Liang, S., Wang, X.-F., and Zhang, D.-P.** (2016).
985 Overexpression of the MYB37 transcription factor enhances abscisic acid sensitivity,
986 and improves both drought tolerance and seed productivity in Arabidopsis thaliana.
987 Plant Mol Biol **90**: 267–279.

988 **Zeng, J., Dong, Z., Wu, H., Tian, Z., and Zhao, Z.** (2017). Redox regulation of plant stem
989 cell fate. EMBO J **36**: 2844–2855.

990 **Zhang, C., Wang, J., Wenkel, S., Chandler, J.W., Werr, W., and Jiao, Y.** (2018).
991 Spatiotemporal control of axillary meristem formation by interacting transcriptional
992 regulators. Development.

993 **Zhang, T.-Q., Lian, H., Zhou, C.-M., Xu, L., Jiao, Y., and Wang, J.-W.** (2017a). A Two-Step
994 Model for de Novo Activation of WUSCHEL during Plant Shoot Regeneration. Plant
995 Cell **29**: 1073–1087.

996 **Zhang, Z., Tucker, E., Hermann, M., and Laux, T.** (2017b). A molecular framework for the
997 embryonic initiation of shoot meristem stem cells. Dev Cell **40**: 264–277.e4.

998 **Zhao, W., Chen, Z., Liu, X., Che, G., Gu, R., Zhao, J., Wang, Z., Hou, Y., and Zhang, X.**
999 (2018). CsLFY is required for shoot meristem maintenance via interaction with
1000 WUSCHEL in cucumber (Cucumis sativus). New Phytol **218**: 344–356.

1001 **Zhao, Z., Andersen, S.U., Ljung, K., Dolezal, K., Miotk, A., Schultheiss, S.J., and**
1002 **Lohmann, J.U.** (2010). Hormonal control of the shoot stem-cell niche. Nature **465**:
1003 1089–1092.

**Zhou, X., Lindsay, H., and Robinson, M.D.** (2014). Robustly detecting differential expression in RNA sequencing data using observation weights. Nucleic Acids Res **42**: e91.

**Zhu, X. et al.** (2014). An efficient genotyping method for genome-modified animals and human cells generated with CRISPR/Cas9 system. Sci Rep **4**: 6420.

## Figure Legends

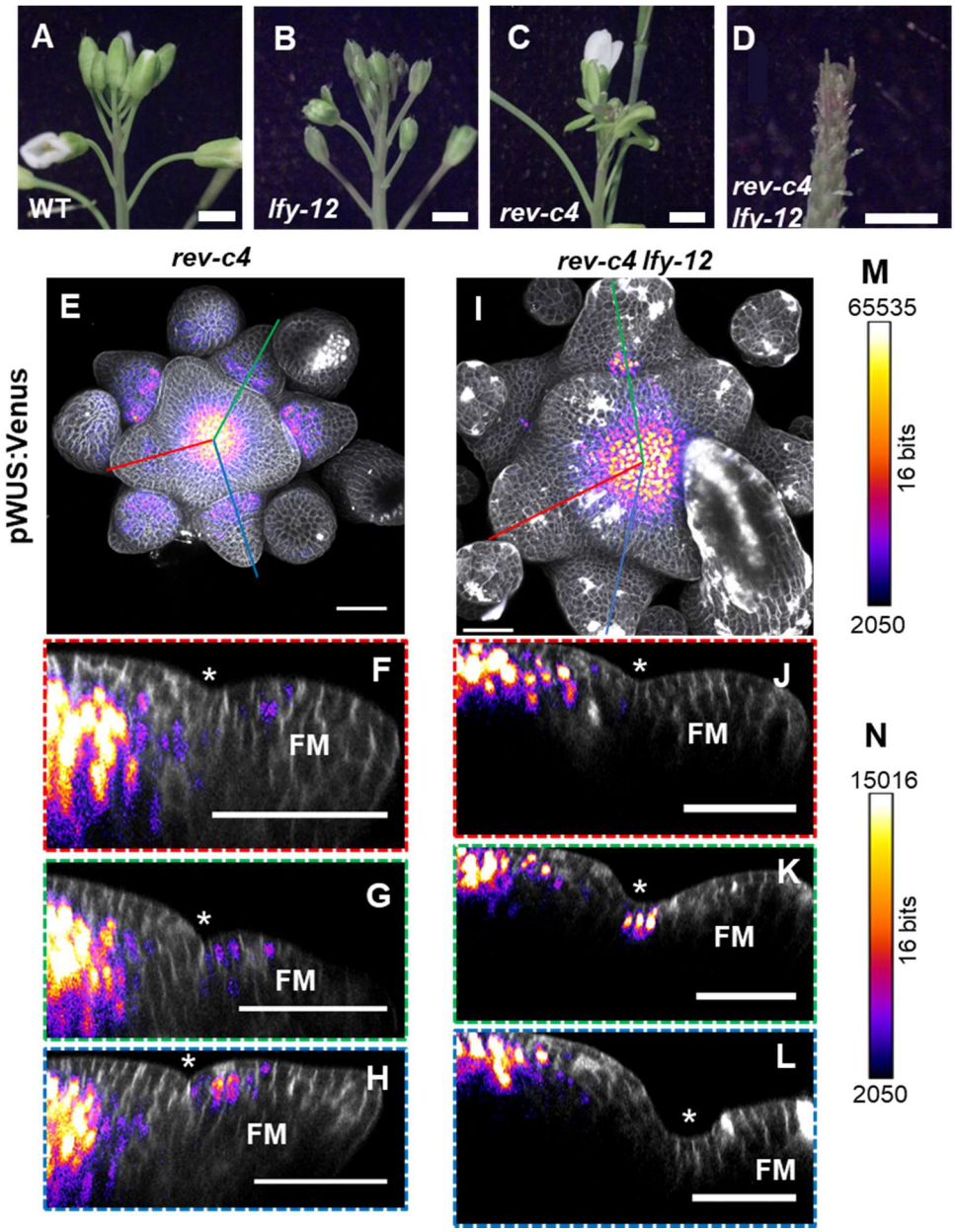


**Figure 1. LFY and REV control floral meristem establishment.**

(A-D) Inflorescences of WT (A; *pWUS:Venus*), *lfy-12* (B), *rev-c4* (C) and *rev-c4 lfy-12* (D) mutants. Flowers of the double mutant are almost entirely replaced by filaments. Scale bar: 1 mm. (E-H) Maximum intensity projection (E, I) and orthogonal cross-sections (F-H, J-L) of confocal z-stacks of wild-type (E-H) and *rev-c4 lfy-12* (I-L) inflorescence meristems expressing the *pWUS:Venus* reporter. The color frames around the cross-sections correspond to the position of the identically colored lines on the projected stacks. The stars indicate the position of the organ axil. Grey: cell-wall staining (propidium iodide), fire heatmap: Venus signal. Scale bars: 50 µm. (M) Intensity heatmap scale for (E,I). (N) Intensity heatmap scale for (F-H, J-L).

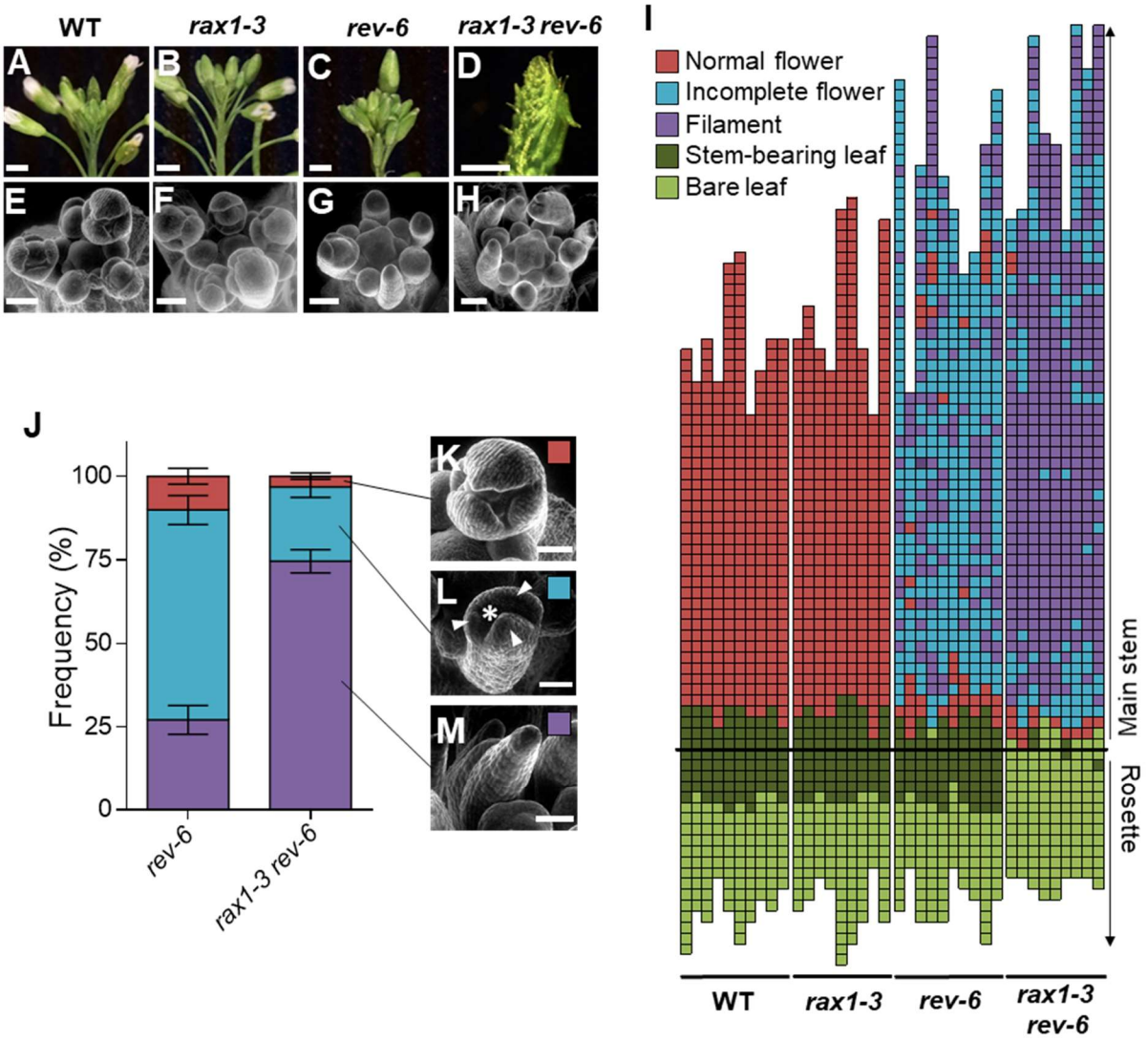


**Figure 2. RAX1 and REV act together to control flower initiation.**

(A-H) Inflorescences of WT (A,E), *rax1-3* (B,F), *rev-6* (C,G) and *rax1-3 rev-6* (D,H) plants, observed by light (A-D; scale bar: 2 mm) or scanning electron microscopy (E-H; scale bar: 100 µm). (I) Plant architecture diagram of WT (Col-0), *rax1-3* and *rev-6* single and double mutants three weeks after bolting. Each column represents an individual plant and each square represents a single internode. Squares below the thick black line represent internodes on the rosette and squares above the thick black line, internodes on the main stem. Structures initiated are color-coded. Dark green: leaf and axillary stem; light green: leaf lacking the axillary stem; red: wild-type flower; blue: flower lacking one or more internal whorls; purple: filamentous structure. (J) Proportion of floral structures initiated in *rev-6* and *rax1-3 rev-6* mutants (N ≥ 9). Close up of the scored structures is shown on the right. Red: normal flower (K), blue: incomplete flower lacking a meristematic dome (star) between developing sepals (arrowheads) (L), violet: filament (M). Scale bar: 100 µm.

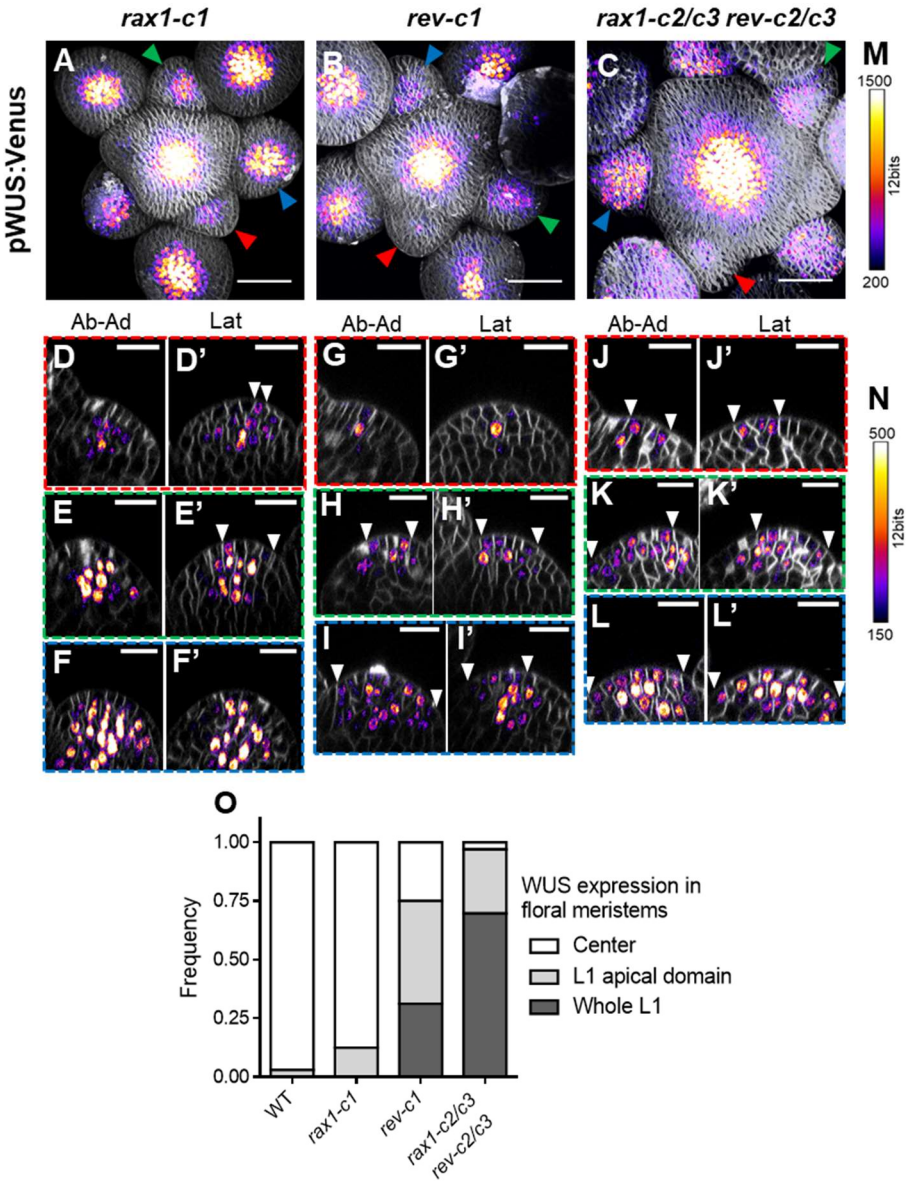


**Figure 3. RAX1 and REV establish flower meristem organization.**

(A-C) Maximum intensity projection of confocal z-stacks of *rax1-c1* (A), *rev-c1* (B) and *rax1-c2/c3 rev-c2/c3* (C) inflorescences expressing the *pWUS:Venus* reporter. Grey: cell-wall staining (FM4-64), fire heatmap: Venus signal. Scale bars: 50 µm. Color arrowheads indicate the position of the primordia cross-sections (D-L') with identically colored color-frames. (D-L') Orthogonal sections through flower primordia across the abaxial-adaxial (left) and lateral (right) axes of the *rax1-c1* (D-F'), *rev-c1* (G-I') and *rax1-c2/3 rev-c2/3* (J-L') plants. White arrowheads mark the limits of *WUS* expression in the L1. Grey: cell-wall staining (FM4-64), fire heatmap: Venus signal. Scale bars: 20 µm. (M) Intensity heatmap scale for (A-C). (N) Intensity heatmap scale for (D-L'). (O) Frequency of flower primordia expressing *WUS* in the central domain only (white), the apical domain of the L1 (light grey), or throughout the L1 (dark grey). N ≥ 23.

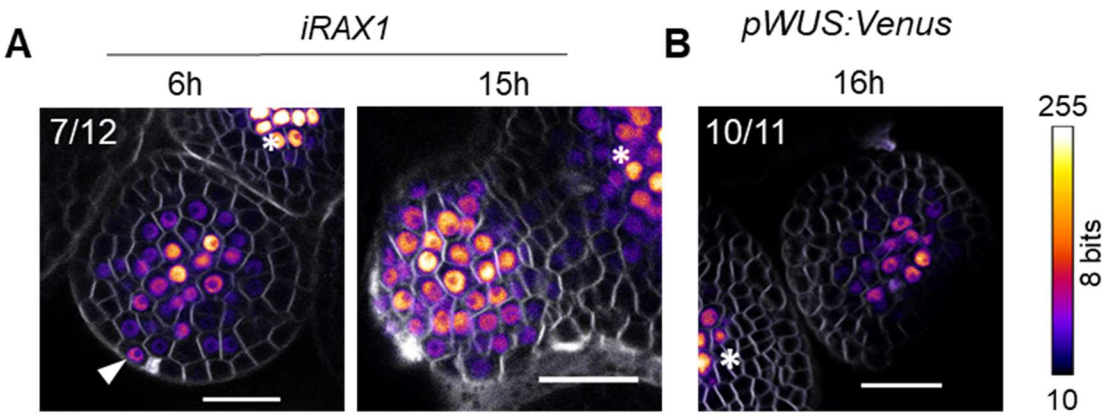


**Figure 4. RAX1 induction leads to activation of *WUS* expression.**

Transverse sections through young flower primordia of *iRAX1i* (A) or wild-type (B) plants carrying the *pWUS:Venus* transgene after DEX treatment. Arrowhead indicates ectopic *WUS* expression in the L1. Stars indicate the position of the SAM. Grey: cell-wall staining (FM4-64), fire heatmap: Venus signal. Scale bars: 20 µm.

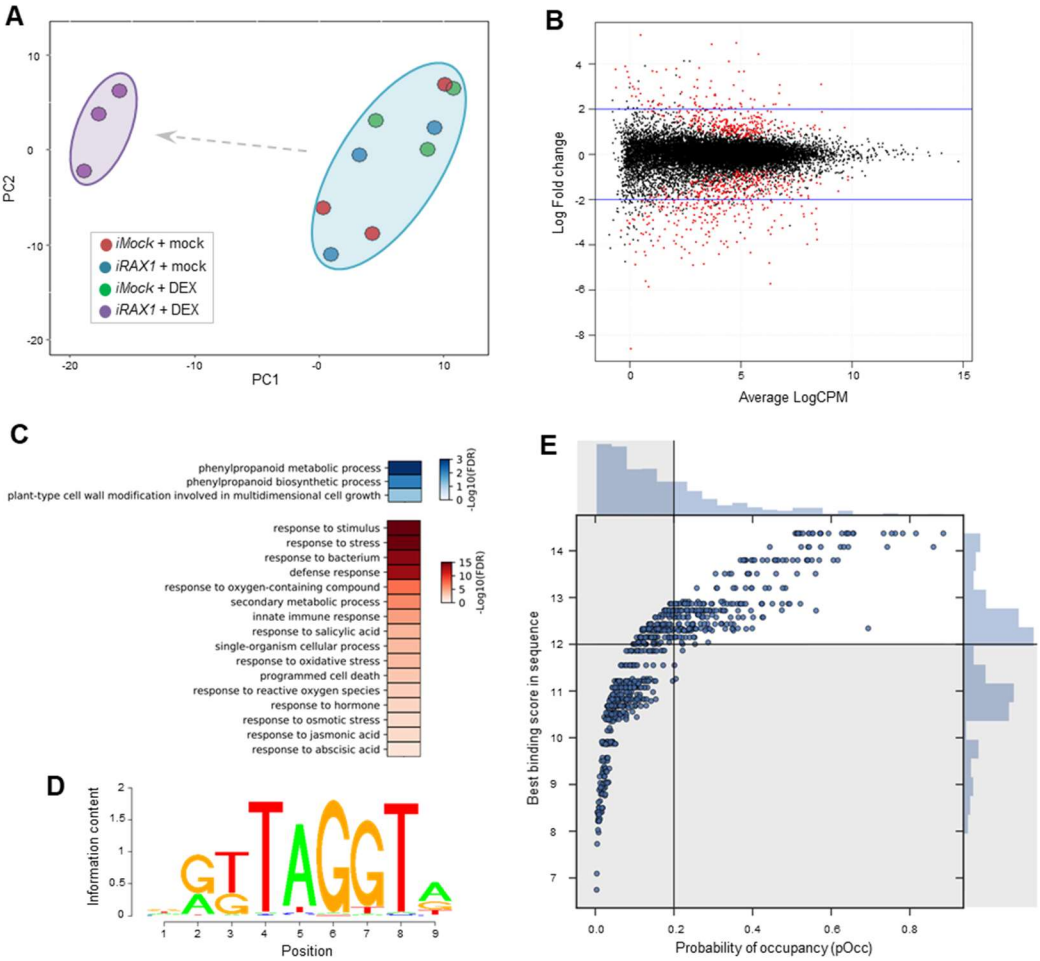


**Figure 5. Identification of RAX1 target genes.**

(A) Principal component analysis of the 500 differentially expressed genes with the highest variance across samples, separated along the two principal components (PC1 and PC2). The non-induced samples (Mock-treated *iRAX1* (blue) and *iMock* (Red) or DEX-treated *iMock* (Green)) segregate together (blue cloud), while the induced RAX1 samples (DEX-treated *iRAX1* (Violet)) are clearly separated. (B) Identification of differentially expressed genes by RNA-seq. The average Log of count per million read (logCPM) is plotted against the Log fold-change (logFC) value across samples for the interaction of genotype:treatment. Differentially expressed genes are indicated in red (FDR ≤ 0.01). (C) Enriched gene-ontology terms amongst up-regulated (blue) and down-regulated (red) genes. FDR ≤ 0.05. (D) DNA-binding model of RAX1 as determined by protein-binding microarray. Letter size indicates the information content at each position of the motif. (E) Identification of potential direct targets of RAX1. The probability of occupancy (pOcc) of RAX1 on each targets genomic sequence is plotted against the best binding score for RAX1 within this sequence. Distribution histograms of the pOcc (top) and best binding score (right) are represented. Targets were selected using a pOcc threshold of 0.2 and a binding score threshold of 12 (bold lines). The other sequences (greyed area) were not considered as potential direct targets.

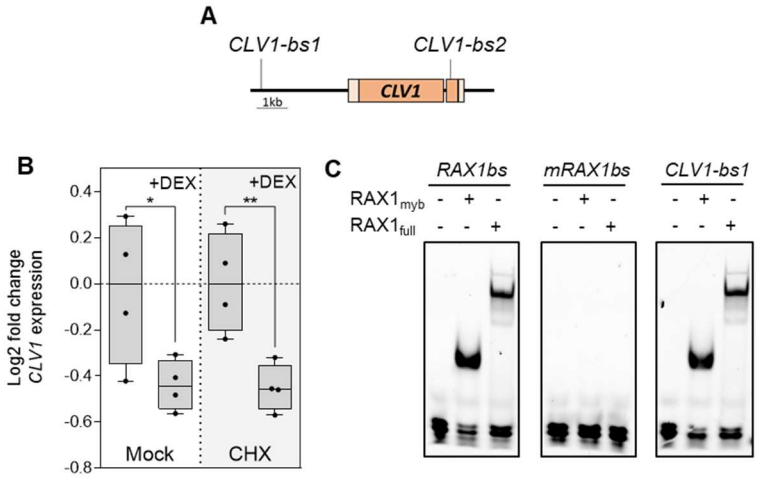


**Figure 6. *CLV1* is a direct target of RAX1.**

(A) Scheme of *CLV1* genomic locus with the two best RAX1 predicted binding site (*CLV1-bs1* and *CLV1-bs2*). Untranscribed regions and introns are indicated by a black line, exons and 5' and 3' UTR are indicated as dark and light orange boxes respectively. (B) Quantification of CLV1 transcripts in *iRAX1* inflorescences treated with mock, dexamethasone (DEX), cycloheximide (CHX) and CHX + DEX. * $p < 0.05$, ** $p < 0.01$, determined by Student's t-test (N = 4). Each point represents a single biological replicate. (C) *In vitro* binding assay of RAX1full and RAX1myb on sequences from *CLV1* genomic region (*CLV1-bs1*), the best possible RAX1 binding site according to the DNA-binding model (*RAX1bs*) and a mutated version of this binding site (*mRAX1bs*).